

Det Kongelige Danske Videnskabernes Selskab

Matematisk-fysiske Meddelelser, bind **30**, nr. 11

Dan. Mat. Fys. Medd. **30**, no. 11 (1955)

*DEDICATED TO PROFESSOR NIELS BOHR ON THE  
OCCASION OF HIS 70TH BIRTHDAY*

MULTIPOLE ORDER  
OF THE  $\gamma$ -RAYS FROM  ${}_{81}\text{Tl}^{208}$

BY

O. B. NIELSEN



København 1955

i kommission hos Ejnar Munksgaard

Printed in Denmark  
Bianco Lunos Bogtrykkeri A-S

The internal conversion lines originating in excited levels of  ${}_{81}\text{Tl}^{208}$  have been obtained in coincidence with  $\alpha$ -particles from  ${}_{83}\text{Bi}^{212}$ . Five of the transitions were found to be magnetic dipole from their internal conversion coefficients. In three cases, the multipole order was confirmed by the  $K/L$  ratios.

The results are compared with the model of PRYCE<sup>3)</sup>.

## 1. Introduction.

In the *Th*-active deposit,  ${}_{81}\text{Tl}^{208}$  is formed by the  $\alpha$ -decay of  ${}_{83}\text{Bi}^{212}$ . The  $\alpha$ -spectrum consists of six lines, and the corresponding level scheme is of particular interest since  ${}_{81}\text{Tl}^{208}$  has one proton hole and one neutron outside a double-closed shell structure.

The levels as indicated by the  $\alpha$ -spectrum appear in Fig. 1. From shell model considerations, PRYCE<sup>3)</sup> has interpreted the two lowest levels as a doublet resulting from the splitting of an  $(s_{1/2} g_{9/2})$  configuration. Similarly, the four upper levels can be obtained by the splitting of a  $(d_{3/2} g_{9/2})$  configuration. Tentatively, the angular momenta shown in Fig. 2 were ascribed to the levels.

The  $(\alpha-\gamma)$  angular correlation measurements of HORTON and SHERR<sup>4)</sup>, and of WEALE<sup>5)</sup>, suggest that the angular momenta of the ground state and the first excited level are  $(5, 4)$ . This agrees with the subsequent disintegration of  $\text{Tl}^{208}$ , which decays by  $\beta$ -emission ( $\log ft \sim 5.5$ ) to levels with angular momenta  $5^-$  and  $4^-$ , but not to the  $3^-$  level in  ${}_{82}\text{Pb}^{208}$ <sup>6)</sup>. A determination of the multipole order of the  $\gamma$ -rays from the excited levels would provide a further test on the consistency of the assignments of Fig. 2. As the total excitations of the different levels are known with great accuracy from the  $\alpha$ -spectrum, the internal conversion coefficients for the  $\gamma$ -transitions can be found merely from the absolute intensity of the  $\beta$ -lines.

The disintegrations taking place in the *Th*-active deposit are shown in Fig. 3. Several of the lines in the composite  $\beta$ -ray spectrum are known to originate in  $\text{Tl}^{208}$ . The decay of the 40 keV level to the ground state thus results in the very strong *L*, *M*, and *N* conversion lines which, by ELLIS<sup>2)</sup>, were denoted the *A*, *B*, and

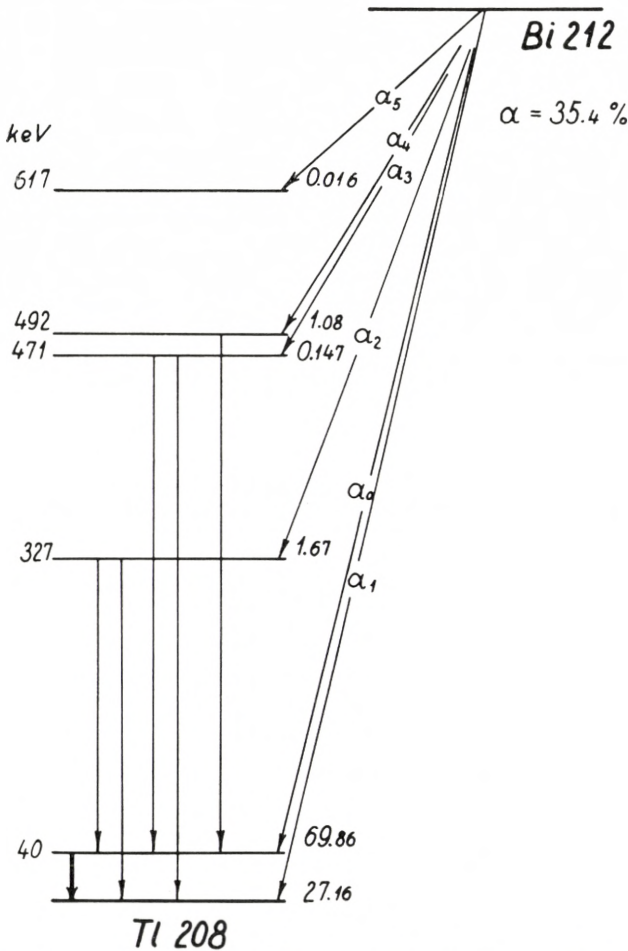


Fig. 1. The decay scheme  $Bi^{212} \rightarrow Tl^{208}$ . The numbers to the right in the figure indicate the excitation of the levels according to RYTZ<sup>1)</sup>. The energies are as found by ELLIS<sup>2)</sup>. Transitions observed in this investigation are shown by vertical arrows.

$B_b$  lines. The radiation has been established to be of  $M1$  nature from the  $L_I:L_{II}:L_{III}$  ratio and from the lifetime<sup>7)</sup>. The other lines are much weaker, as can be seen from Fig. 1. The  $K$ -conversion line for the transition from the 327 keV level to the 40 keV level (in ELLIS' notation the  $G_a$  line) has been measured by FLAMMERSFELD<sup>8)</sup>. Some other lines have been recorded on photographic plates<sup>2)</sup>, but their intensities are not known with sufficient accuracy.

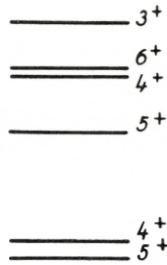


Fig. 2. The angular momenta proposed by PRYCE<sup>3)</sup>. The value 6 for the 5th level is not in accordance with experiment.

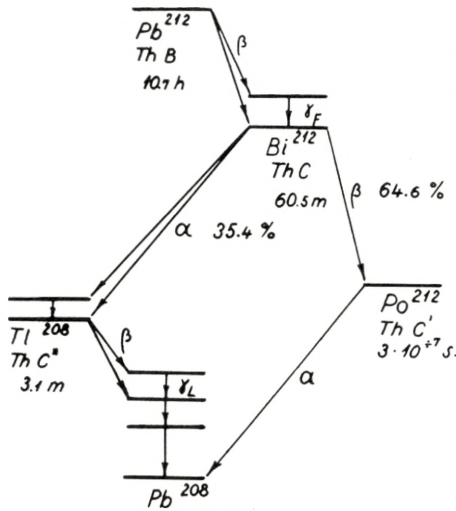


Fig. 3. Decays taking place in the Th-active deposit. Only the stronger branches are shown.

The experimental difficulties are due partly to the continuous  $\beta$ -ray background, partly to numerous strong lines from transitions in  $Bi^{212}$  and  $Pb^{208}$ . The investigation described here represents an attempt to overcome these difficulties by utilizing the coincidence between the  $\beta$ -particles and the internal conversion lines.

### 2. The Spectrometer.

The  $\beta$ -ray spectrometer<sup>9)</sup> which we have recently constructed is especially well suited for coincidence experiments of this type. A 30 mm dia. glass plate covered with a thin layer of ZnS powder

was placed immediately behind the source. The glass plate was optically coupled to the photocathode of a multiplier tube RCA 6199 through a vacuum tight lucite window.

This type of counter produces rather strong pulses when hit by  $\alpha$ -particles, and gives practically no response to  $\beta$ - and  $\gamma$ -radiation.

The transmission of the spectrometer without the  $\alpha$ -counter is about 9 per cent, at a resolution of  $\frac{1}{R} \sim 1.5$  per cent. It proved advantageous to place the  $\alpha$ -counter so near the source that it covered a fraction of the useful solid angle of the spectrometer, which reduced the transmission to about 8 per cent. More than 35 per cent of the  $\alpha$ -particles could then be counted, and the efficiency in the coincident spectrum was between 2.5 and 3 per cent.

$\beta$ -particles focused in the spectrometer were counted by an anthracene crystal with optical coupling to a multiplier, EMI 6260. The voltage supplied to this photo multiplier tube was varied so as to give pulses of the same height for all energies of the  $\beta$ -particles.

The pulses from the two counters were fed through cathode followers to a coincidence stage with variable resolving time. The counts from the anthracene crystal and the coincidences were recorded on two decade scalars. The magnetic field had only negligible effect on the efficiency of the counters.

For reasons which will be referred to later, it was necessary to use rather strong sources. Usually, the  $\alpha$ -counter was hit by about  $10^5$   $\alpha$ -particles per second. Although  $ZnS$  is a slow phosphor with a decay time of several  $\mu s$ , a proper shaping of the pulses reduced the blocking of the circuit caused by each pulse to about 1  $\mu s$ , but the dead time still amounted to about 10 per cent. It was found that the rate of true and random coincidences was reduced to the same extent, and also that the dead time corrections varied with the source strength as predicted by counting theory. The coincidence resolving time was of the order of  $1/10 \mu s$ . It could not be reduced very much below this without loss of true coincidences, presumably because of the slowness of the  $ZnS$  phosphor.

### 3. The Sources.

The sources were prepared by activation in *Th*-emanation of small bits of aluminum foil with a thickness of  $150 \mu\text{g}/\text{cm}^2$ . In most cases, these were placed between two larger pieces of the same foil and then fixed to a frame of thin copper wire by means of a small amount of vacuum grease. This mounting of the source prevents the escape of recoiling radioactive atoms, an effect described in more detail by FLAMMERSFELD<sup>8)</sup>.

Uncovered sources were used for the measurement of lines with energy below 100 keV, and the foils were activated on one side only. The counting of particles having passed through the foil had also to be avoided in these cases, and only three of the gaps of the spectrometer could be utilized.

### 4. The Coincident Spectrum.

#### *a. Background conditions.*

Both the composite spectrum, consisting of all the  $\beta$ -rays from the *Th*-active deposit, and the  $\alpha$ -coincident part of it were recorded during the measurements. The correction factor for random coincidences was found simply from the strength of a non-coincident line in the coincident spectrum. For this purpose the *F*-line, the very strong *K*-conversion line for the 238 keV transition in  $\text{Bi}^{212}$  (see Fig. 3), was generally used. For some different points of the line the number of coincidences was plotted against the total counts. A straight line was then obtained, and the slope giving the correction factor could be found in a few minutes with a statistical uncertainty less than two per cent. Random coincidences were normally less than one per cent of the counts in the composite spectrum.

Fig. 4 shows the final spectrum corrected for random coincidences. The continuous background is due to  $\beta$ -particles in coincidence with  $\alpha$ -particles from  $\text{Po}^{212}$  (see Fig. 3). Since the half life of this isotope is only about  $^{3/10} \mu\text{s}$ , a fraction of the  $\alpha$ -particles is emitted so fast that they appear coincident with the  $\beta$ -particles in the continuous spectrum from  $\text{Bi}^{212}$ . With a resolving time  $\sim ^{1/10} \mu\text{s}$ , about 8 per cent of these  $\alpha$ -particles

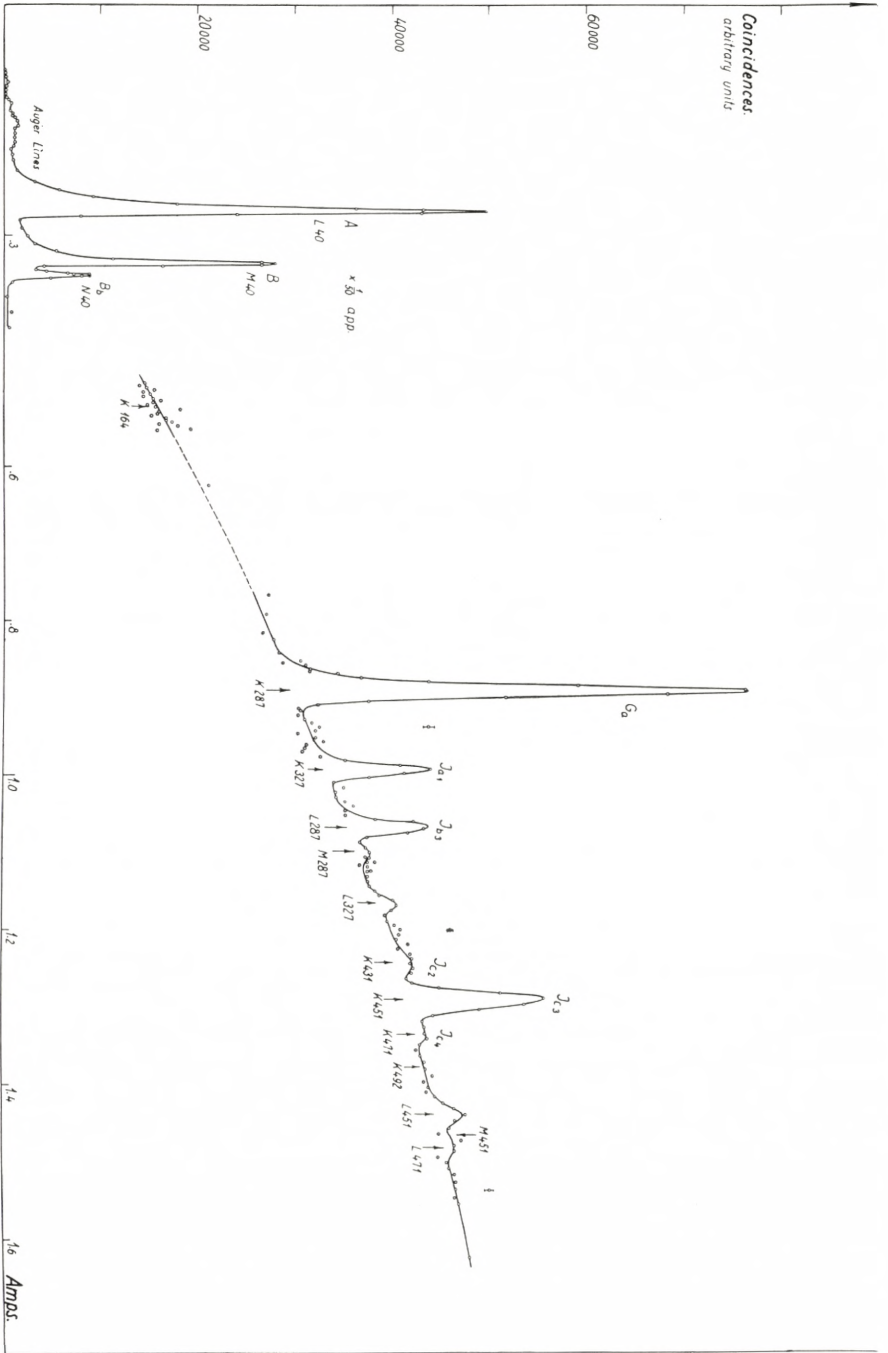


Fig. 4. The coincident spectrum. The lines observed by Ellis<sup>21</sup> are denoted by the letters introduced by him. The terms below the curve refer to conversion shell and  $\gamma$ -ray energy, the arrows indicating the calculated positions of the lines. Standard statistical fluctuations are indicated by dotted bars above the curve.



were able to produce coincidences, and this background constituted the main experimental difficulty.

If a background consists principally of random coincidences, it varies approximately as the second power of source strength. The outcome of an experiment will then be rather independent of the source strength, since the height of the coincident lines as well as the statistical fluctuations go with first power. This does not hold for the background described above. Sufficient statistical accuracy could be obtained within a reasonable time only when the sources were as strong as possible, the limiting factor being the dead time of the coincidence circuit.

In order to cover a reasonable part of the spectrum within the half life of the source, 10.7 h, counting could not go on more than 10 min. for each point. With this counting period the height of the weaker lines was less than twice the statistical fluctuations. To improve the accuracy, the measurements were repeated, for a certain part of the spectrum 13 times. The magnetic field was adjusted to the same values in each run to make possible a summation of the statistical material.

The spectrum on Fig. 4 contains a summary of the information gained from these experiments. Standard statistical deviations for the different parts are given by the dotted bars above the curve. The section between the arrows M 287 and K 492 was measured with the greatest accuracy, each point corresponding, as mentioned, to more than two hours of counting. Then the three weak lines in the region had a height of more than 6 times the statistical fluctuations. The spectrum represents more than 200 hours of measurements.

#### *b. The strength of the lines.*

Of the stronger lines in Fig. 4,  $B$  and  $J_{c3}$  are completely resolved from non-coincident lines in the composite spectrum. The ratio between their intensities in the two spectra could then be found, thus giving the efficiency of the coincidence arrangement. The results obtained from both lines agreed. Unfortunately,  $J_{c3}$  is not strong enough to make the experimental uncertainty less than about 10 per cent, but the relative strength of neighbouring lines is certainly given with rather good accuracy from Fig. 4.

The determination of the absolute intensities involves a comparison in the composite spectrum of the area under at least one of them with the total area of the continuous  $\beta$ -ray spectra, which represents the total number of disintegrations in the source. The line  $G_a$  has been measured in this way by FLAMMERSFELD<sup>8)</sup>, unfortunately, however, with poor statistical accuracy.

The composite spectrum recorded simultaneously with the coincident part could in principle be used in this manner. It appeared, however, that the scattering of particles caused by the  $\alpha$ -counter increased the area of the continuous spectrum between 15 and 20 per cent. The general shape was not changed very much, and neither the shape nor the relative strength of the lines was altered. As a number of the stronger lines have been measured absolutely with great care in other cases<sup>8,10,11)</sup>, the intensity of the coincident lines could also have been found merely by using these known lines as standards instead of the continuous spectrum.

It was decided, however, to make an independent determination on the  $G_a$  line. As a check of the reliability of the procedure, a few of the strong lines with known intensity were redetermined. These measurements, performed with the  $\alpha$ -counter removed, are described in Section 5.

## 5. Redetermination of the Intensity of $G_a$ and Some Strong Lines.

### *a. The F and L lines.*

The area of the continuous  $\beta$ -ray spectra was obtained by the procedure worked out by FLAMMERSFELD<sup>8)</sup> and others<sup>10)</sup>. To diminish the uncertainties from the measurement of the low energy  $\beta$ -rays, the method makes use of only the partial spectra of high energy which originate in  $Bi^{212}$  and  $Tl^{208}$  (Fig. 3). The separation from the soft component of  $Pb^{212}$  was made by extrapolation, according to the spectral shape for  $(Bi^{212} + Tl^{208})$  as found by FLAMMERSFELD<sup>8)</sup> and by MARTIN and RICHARDSON<sup>10)</sup>.

Due to the one hour lifetime of  $Bi^{212}$  compared to the 10.7 hour lifetime of  $Pb^{212}$ , the  $(Bi^{212} + Tl^{208})$ -spectrum must be approximately 11 per cent stronger than the spectrum of  $Pb^{212}$  when the source is in radioactive equilibrium<sup>10)</sup>.

The two strong lines,  $F$  (148 keV) and  $L$  (422 keV), representing different energy regions, were selected. They were obtained with the same resolution as used in the coincident measurements.

The intensity of  $F$  was found to be  $0.30 \pm 0.02$  of all disintegrations  $Pb^{212} \rightarrow Bi^{212}$ . This is in accord with more recent determinations<sup>8, 10, 11</sup>). The measurement was reproducible within 2 per cent, but the experimental uncertainty must be estimated as somewhat higher, due to some arbitrariness in the method of extrapolating.

The ratio between the intensities of the  $F$  line and the  $L$  line was found to be  $45 \pm 3$ , in agreement with MARTIN and RICHARDSON. FLAMMERSFELD has found a ratio of 37, but his results seem to be higher than other determinations for several of the high energy lines.

#### *b. The $G_a$ and $I$ lines.*

As mentioned previously, the coincident lines  $B$  and  $J_{c3}$  are not disturbed by neighbouring lines, and their intensities could thus be deduced from a comparison with the  $F$  line.  $J_{c3}$  is rather weak, however, and the energy of the  $B$  line (36 keV) is so low that a certain loss of true coincidences could not be excluded. Therefore, it was decided to base the determination of the absolute strength of the coincident lines on  $G_a$  (202 keV). With the resolution used in the experiments described so far, this line was not resolved from the very much stronger  $H$  line from  $Bi^{212}$ , which has a momentum only 2 per cent higher. Consequently the resolution was increased to  $\frac{1}{R} \sim 0.7$  per cent. Only two of the gaps of the spectrometer were utilized, with the solid angle reduced to  $\sim 1.5$  per cent. The source was about  $3 \times 1$  mm<sup>2</sup>, and the transmission was then 1.2 per cent.

Fig. 5 shows the  $G$ ,  $G_a$ , and  $H$  lines which are well resolved at this resolution. The height of  $G_a$  relative to  $F$  could be found with a statistical uncertainty not exceeding 2 per cent, but the experimental uncertainty was raised somewhat due to the tail of the  $H$  line, which contributed to the strength of  $G_a$  by a few per cent.

With the intensity of the  $F$  line as given above, the strength

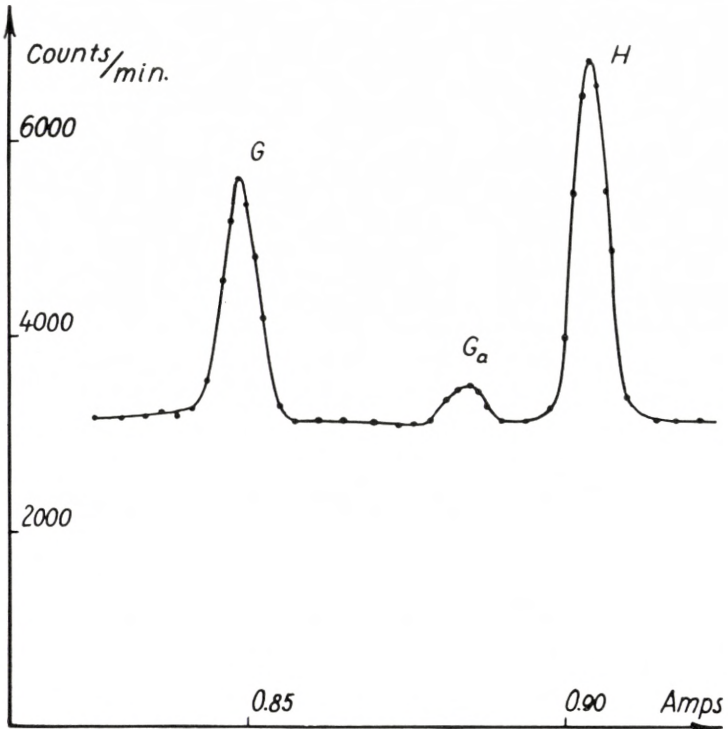


Fig. 5. The  $G$ ,  $G_a$ , and  $H$  lines. Resolution 0.7 per cent.

of  $G_a$  was found to be  $(11.3 \pm 1.2) \times 10^{-4}$  of all disintegrations of  $Bi^{212} + Tl^{208}$ . This agrees with FLAMMERSFELD's<sup>8)</sup> results.

At this resolution, the  $I$  line also is separated from the neighbouring lines. The ratio  $\frac{F}{I}$ , which is the  $K/L$  ratio for the 238 keV magnetic dipole<sup>7)</sup>  $\gamma$ -ray, was determined to  $5.5 \pm 0.2$ , also in accordance with FLAMMERSFELD.

## 6. The Multipole Order of the Transitions.

The 40 keV transition responsible for the strong low energy lines in Fig. 4 is known to be of M1 nature<sup>7)</sup>. An accurate determination of the intensity of these lines was not attempted, but it was found that internal conversion took place in more than

70 per cent of the cases. A better determination of the conversion coefficients has been obtained from measurements of the  $\gamma$ -ray<sup>5, 12)</sup>.

From Fig. 4, in addition to the low energy lines, 5 *K*-conversion lines and 3 *L*-conversion lines can be established. The intensities are roughly in agreement with the results of ELLIS<sup>2)</sup> for the lines  $G_a$ ,  $J_{a1}$ , and  $J_{b3}$ , but  $J_{c2}$  turned out to be two times weaker and  $J_{c3}$  four times stronger than previously reported. It is remarkable that the lines L 327 and L 451 have not been observed earlier, although they are stronger than  $J_{c2}$  and  $J_{c4}$ . The strength of the lines on Fig. 4, relative to  $G_a$ , is given in Table I.

TABLE I.

$\gamma$ -ray energy keV.	Conv. shell	$\beta$ -line energy keV.	Intensity relative to $G_a$	$\gamma$ -ray energy keV.	Conv. shell	$\beta$ -line energy keV.	Intensity relative to $G_a$
287	K	202	1	431	K	346	$0.035 \pm 0.010$
287	L	272	$0.19 \pm 0.01$	451	K	366	$0.30 \pm 0.02$
327	K	242	$0.24 \pm 0.01$	451	L	436	$0.055 \pm 0.010$
327	L	312	$0.050 \pm 0.010$	471	K	386	$0.022 \pm 0.006$

Table II shows the corresponding *K*-shell internal conversion coefficients  $\alpha_k$ , and the *K/L* ratios. The calculation is based on  $G_a = 11.3 \times 10^{-4}$ , a branching ratio<sup>13)</sup>

$$\frac{Bi^{212} \rightarrow Tl^{208}}{Bi^{212} \rightarrow Tl^{208} + Po^{212}} = 0.354,$$

and an excitation of the levels as indicated on Fig. 1. In the two cases where two transitions take place from the same level, only a mean value  $\frac{\beta_1 + \beta_2}{\gamma_1 + \gamma_2}$  of the conversion coefficients can be calculated, as the relative intensities of the  $\gamma$ -rays are unknown.

The theoretical conversion coefficients are taken from the tables of ROSE et al.<sup>14, 15)</sup>.

The lifetimes of the excited states must necessarily be of the order of or shorter than the coincidence resolving time,  $1/10 \mu s$ . This excludes multipole orders higher than E1, E2, M1, and M 2, and the conversion coefficients are very different in these cases. The M 1 nature of the transitions in Table II is indicated

TABLE II.

$\gamma$ -Ray energy keV	$\alpha_k$ observed	$\alpha_k$ theoretical				$K/L$ ratios observed	$K/L$ ratios theoretical	
		E1	E2	M1	M2		E2	M1
287	$0.33 \pm 0.05$	0.027	0.070	0.50	1.55	$5.3 \pm 0.3$	1.2	5.7
327		0.020	0.053	0.35	1.00		$5 \pm 1$	1.6
431	$0.14 \pm 0.05$	0.011	0.030	0.17	0.44	$5 \pm 1$	2.5	5.7
471		0.0090	0.024	0.13	0.33			
451	$0.10 \pm 0.02$	0.010	0.027	0.15	0.38			

by the conversion coefficients, and for three of them it is confirmed by the  $K/L$  ratio. The deviations from the theoretical values are probably due to an admixture of E2 radiation\*).

It was not possible to detect the  $K$ -lines for transitions from the 492 keV level to 327 keV or to the ground state. An upper limit for their strength is about  $1/20$  of the line K 451. The excitation of the 617 keV level is about 9 times weaker than for 471 keV. It was not attempted to find the corresponding lines.

## 7. Discussion.

The decay scheme in Fig. 1 is definitely born out by the establishment of coincidences between  $\alpha$ -particles and the internal conversion lines. Change in angular momenta of  $\Delta I = 0$  or 1 are indicated by the magnetic dipole character of the transitions, which also shows the 5 lower levels to have the same parity.

Thus, the angular momenta of the 327 and 471 keV levels must be either 4 or 5 if the ground state doublet, as supported by earlier experiments, is assumed to be (5, 4). The 492 keV level then most probably has angular momentum 3. A low angular momentum for this level is consistent with the relative intensities of the  $\alpha$ -lines.  $Bi^{212}$  has angular momentum 1<sup>4)</sup>, and the  $\alpha$ -transition to the 492 keV level is the most favoured of the transitions shown in Fig. 1. An angular momentum of 3 for this

\*) Note added in proof: Results recently obtained in Amsterdam suggest that the theoretical M1 conversion coefficients are 30-40 per cent too high. G. J. NIJGH and A. H. WAPSTRA: To be published.

level is in disagreement with the assignments of Fig. 2. This is not a serious failure of the model which does not definitely give the order of the levels in a configuration.

### Acknowledgements.

The author wishes to express his sincere gratitude to Professor NIELS BOHR for his continuous interest in these problems and for ideal working conditions in his Institute.

I am indebted to Professor M. H. L. PRYCE for helpful suggestions, and to Drs. AAGE BOHR and BEN R. MOTTELSON for valuable discussions.

*Institute for Theoretical Physics,  
University of Copenhagen,  
Denmark.*

---

## References.

1. A. RYTZ: C. R. **233**, 790 (1951)
2. C. D. ELLIS: Proc. Roy. Soc. **A 138**, 318 (1932)
3. M. H. L. PRYCE: Proc. Phys. Soc. **65 A** 773, **65 A**; 962, (1952)
4. J. HORTON and R. SHERR: Phys. Rev. **90**, 388 (A) (1953)
5. J. W. WEALE: Proc. Phys. Soc. **68 A**, 35 (1955)
6. L. G. ELLIOT, R. L. GRAHAM, J. WALKER, and J. L. WOLFSON: Phys. Rev. **93**, 356 (1954)
7. R. L. GRAHAM and R. E. BELL: Can. Jour. of Phys. **31**, 377 (1953)
8. A. FLAMMERSFELD: Z. Phys. **114**, 227 (1939)
9. O. B. NIELSEN and O. KOFOED-HANSEN: Dan. Mat. Fys. Medd. **29**, no. 6 (1955)
10. D. G. E. MARTIN and H. O. W. RICHARDSON: Proc. Roy. Soc. **A 195**, 287 (1948)
11. N. FEATHER, J. KYLES, and R. W. PRINGLE: Proc. Phys. Soc. **61**, 466 (1948)
12. B. B. KINSEY: Phys. Rev. **72**, 526 (1947)
13. P. MARIN, G. R. BISHOP, and H. HALBAN: Proc. Phys. Soc. **66 A**, 608 (1953)
14. M. E. ROSE, G. H. GOERTZEL, and C. L. PERRY: ORNL-1923 (1953)
15. M. E. ROSE, G. H. GOERTZEL, and C. SWIFT: L-shell internal conversion coefficients, privately distributed.